# FERMILAB'S EXPERIENCE WITH A HIGH-ENERGY ELECTRON COOLER*

L.R. Prost# and S. Nagaitsev, FNAL, Batavia, IL 60510, U.S.A.

*Abstract*

The Recycler ring at Fermilab served as a repository of 8 GeV antiprotons destined for collision in the Tevatron, a proton-antiproton collider. From 2005 to 2011, the world's only relativistic electron cooling system was used to cool the antiprotons for accumulation and preparation of bunches before injection into the collider ring.

With a 4.3-MeV, 0.1-A DC electron beam, a weak continuous longitudinal magnetic field in the cooling section and lumped focusing elsewhere, this unique electron cooler allowed for significant improvements in the Tevatron luminosity, yet also presented numerous challenges, such as achieving reliable operation of a high-voltage, high-power electrostatic accelerator in a high-current recirculation mode. In this paper, we discuss the experience of running this unique machine.

## INTRODUCTION

The missions for the cooling systems in the Recycler were to neutralize multiple Coulomb scattering (IBS and residual gas), neutralize the effects of heating due to the Main Injector ramps (stray magnetic fields), reduce the emittances of the stored antiprotons between transfers from the Accumulator and reduce the phase space of the stored antiprotons in preparation for a Tevatron store. To this end, an electron cooler was envisioned as an important part of the Recycler ring upgrade and discussed in the original Recycler Technical Design Report [1].

Installation of the Recycler Electron Cooler (REC) was completed in February 2005, relativistic electron cooling demonstrated within 6 months [2], and put into operation days later. By the end of the Tevatron collider Run II in October 2011, electron cooling had significantly contributed to the several-fold increase of the luminosity production.

## CHOICE OF THE SCHEME

All coolers that had been built previously worked at non-relativistic energies ($E_e < 300$ keV). They used a strong (~1 kG) longitudinal magnetic field to transport the electron beam and enhance the cooling force. With a typical requirement of tens of minutes for the cooling time, a scheme without a strong magnetic field in the cooling section (a.k.a. non-magnetized cooling) was shown to be satisfactory at a reasonable electron beam current (~0.5 A).

The non-magnetized approach is a clear deviation from the way coolers are being built, and it brought up serious questions about the stability of the electron beam transport and ability to provide low transverse electron velocities in the cooling section. A novel approach was devised [3] in which the electron gun and the cooling section are both immersed in a longitudinal magnetic field but beam focusing in between is provided by separate solenoid lenses. However, a beam generated inside a solenoid and extracted into free space acquires an effective rms normalized emittance (in the paraxial ray approximation):

$$\varepsilon_{B,eff} = \frac{eB_{cs}R_{cs}^2}{8m_e c^2}$$

where $B_{cs}$ is the magnetic field in the cooling section, $R_{cs}$ is the beam radius, $e$ and $m_e$ are the electron charge and mass, and $c$ the speed of light. This emittance arises from the conservation of the canonical angular momentum, which in turn results in a coherent angular rotation of the beam and needs to be taken into consideration in the design of the transport beam lines optics. To accommodate lumped focusing at low $\gamma$ during acceleration, the beam size, $R_{cs}$, and magnetic field, $B_{cs}$, in the cooling section were limited to 2-4 mm and 100-200 G, respectively.

Based on preliminary cooling scenarios and estimations of the cooling rates, design parameters were specified [4] (they are partly reproduced in Table 1). Table 1 assumes a scheme with a DC electron beam, a longitudinal magnetic field at the cathode and in the cooling section, and lumped focusing in the beam transport lines (description of the cooler setup can be found in Ref [5] for instance). Table 1 also shows typical beam parameters during regular operation (when the electron beam was fully optimized).

Table 1: Parameters of the Cooler

| Parameter | Unit | Design | Operation |
|---|---|---|---|
| Electron energy | MeV | 4.33 | 4.33 |
| Beam current, DC | A | 0.5 | 0.1 |
| Terminal voltage ripple (rms) | V | 500 | ~150† |
| Magnetic field at the cathode | G | ≤ 600 | 86 |
| Magnetic field in the cooling section | G | ≤ 150 | 105 |
| Electron beam divergence | μrad | 80 | ~100† |
| Pressure | nTorr | 0.1 | 0.3 |
| Cooling section length | m | 20 | 20 |

† Inferred from indirect measurements

It should be noted that the electron beam current used for normal operation, 0.1 A, is not an intrinsic limitation of the cooler, but was found sufficient to provide adequate

* Operated by Fermi Research Alliance, LLC under Contract No. DE-AC02-07CH11359 with the United States Department of Energy
# lprost@fnal.gov



ISBN 978-3-95450-140-3

cooling. In fact, operation at 0.5 A was demonstrated and was the norm early on.

## MAIN CHALLENGES

The main challenges found in the realization of the electron cooler may be divided into two broad categories: generation, stability and reliability of a high power electron beam; maintaining a beam of 'good quality' i.e. with low transverse velocities in the cooling section.

### *Beam Recirculation*

To keep the dissipated energy low while using a MW-range DC beam in the cooling section, the cooler employs the energy recovery scheme. After interacting with the antiprotons, the electron beam returns to the accelerator, Pelletron [6], is decelerated and eventually absorbed in a collector at the kinetic energy of 3.2 keV. At Fermilab, this process is called 'beam recirculation'.

Insufficient stability of the electron beam recirculation was the main obstacle at the R&D and commissioning stages. The energy recovery scheme puts stringent limitations on the total beam loss since the Pelletron chains can only provide up to ~400 μA, which is several orders of magnitude lower than the beam current. Moreover, the allowable beam loss inside the Pelletron tubes is restricted even more: a loss comparable with the current flowing through the tube resistive divider (~40 μA) significantly redistributes the potential along the tube. The resulting change in the beam envelope usually causes even larger losses, and the beam is lost in a matter of milliseconds.

The accumulation of charge on the tube ceramic coming from lost electrons induces partial discharges in the acceleration gaps. These discharges occur all the time with frequency dependent on the tube voltage gradient and amount of beam loss. By itself, a discharge of a single gap cannot significantly change the overall voltage distribution. However, a plasma plume from such discharges may shorten one or several neighbouring gaps. If the unaffected portion of the tube is capable of holding the entire voltage, the gaps charge up again, and the beam does not trip. If the beam envelope modification resulting from the altered voltage distribution is large but induces a beam loss only in the beam line outside of the Pelletron proper, a protection system interrupts the beam and normal operation can be restored in a matter of seconds. Otherwise, the entire tube shortens, causing a full discharge.

Several steps allowed making the cooler an operational system.

- Development of an effective gun [7] which incorporate a negatively biased 'control electrode' shaping the electric field near the emitting area, and eliminating large divergence of the beam at low current. The maximum current achieved was 0.6 A in the full line.
- Development of an effective collector [8] with a transverse magnetic field, which greatly reduces the number of secondary electrons escaping the collector. The typical relative beam loss was $2 \cdot 10^{-6}$ on a low-energy test bench and $1.8 \cdot 10^{-5}$ in the full line. The higher beam loss in longer systems is attributed to electron scattering on the residual gas and Intra Beam Scattering (IBS) [4].
- Increasing the total length of the accelerating tubes by 1/5.
- Decreasing the beam loss to the tubes, primarily by tuning the beam envelope in the deceleration tube to transport out of the Pelletron the electrons escaping from the collector.
- Adjusting the beam envelope in the acceleration tube to keep the beam core far from the tube electrodes in the time of the beam trips. It made a difference in preventing full discharges originating in the acceleration tube.
- High vacuum quality (~0.3 nTorr) in the tubes to limit the production of electrons from secondary ions.
- Protection of the deceleration tube from irradiation in the time of beam trips by using optics with high dispersion in the return line.
- Fast protection circuitry, turning the beam off in 1μs after detecting a Pelletron voltage drop of more than 5 kV or other abnormal conditions.

The implementation of these measures allowed operating typically with only several beam trips per day and full discharges as rare as once a year.

### *Beam energy Absolute Calibration and Stability*

Because of slow cooling times, the interaction of the electrons with the antiprotons is not observable if the energy error between the two beams is larger than ~0.1%. The electron energy is mainly determined by the terminal potential. After assembling the Pelletron, the Generator Volt Meter (GVM) was calibrated, first with a 100 kV external power supply and a calibrated resistive divider, and then, by measuring the length of a Larmor spiral pitch in the cooling section [9] at the energy close to the nominal. The resulting change of the GVM calibration was 5.2% with estimated errors of ~0.2%. It was sufficiently low to observe the first interaction between beams. The electron energy was found to be within 3 keV (~0.07%) of its optimal value.

However, once set, the beam energy would fluctuate (or drift), hence degrading cooling efficiency.

Mainly, four mechanisms were identified for having the largest impact on the beam energy:

- Sensitivity of the GVM preamplifier to variations of the building temperature.
- Fluctuation of the distance between the terminal and the GVM due to variations of the Pelletron temperature. An illustration of the magnitude of this dependence is shown on Fig. 1a.
- Insufficient gain of the analogue feedback loop (e.g.: in case of drifts of the chain current).

ISBN 978-3-95450-140-3

- Effect of the insulating gas ($SF_6$) permittivity changes on the GVM readings due to pressure variations.

These effects were minimized by a better control of the temperatures where applicable, and two software loops.

One of them adjusts the chain current to eliminate the difference between the set point of the terminal voltage and its read-back. The second software (a.k.a. energy regulation loop) modifies the set point of the terminal voltage in order to keep the beam position constant in a high-dispersion region, effectively maintaining the beam energy constant.

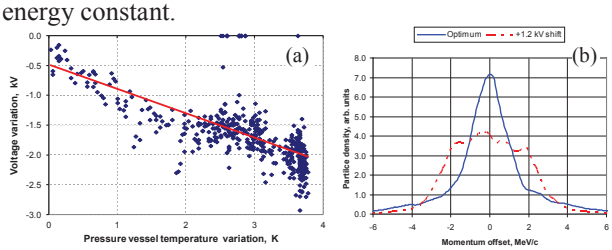


Figure 1: (a) Beam voltage variation vs. tank temperature (slope: -0.4 kV·K$^{-1}$); (b) Momentum distributions of the antiproton beam. Red line: energy offset by 1.2 keV with respect to optimum; Blue line: optimum tuning of the electron beam energy.

## *Beam Quality*

In the non-magnetized cooling model, a heavy charged particle moving in a free electron gas with a velocity distribution $f_e(\vec{v}_e)$ experiences a friction force that in a model of binary collisions can be written following Ref. [10]:

$$\vec{F}_b(\vec{V}_p) = -\frac{4\pi e^4 n_{eb}}{m_e}\eta\int \Lambda_C \frac{f_e(\vec{v}_e)}{(\vec{V}_p-\vec{v}_e)^2}\frac{\vec{V}_p-\vec{v}_e}{\left|\vec{V}_p-\vec{v}_e\right|}d^3v_e \quad (1)$$

where $n_{eb}$ is the electron density in the beam rest frame, $m_e$ the electron mass, $e$ the elementary charge, $\vec{V}_p$ the velocity of the heavy particle, and $\eta = L_{cs}/C$ indicates the portion of the ring circumference $C$ occupied by the cooling section of length $L_{cs}$. $\Lambda_c$ is the so-called Coulomb logarithm.

Assuming Gaussian distributions for all velocity components for both electrons ($\sigma_e$) and antiprotons ($\sigma_p$), a constant Coulomb logarithm, the transverse emittances/velocities to be equal (for both the electron, $\sigma_{ex} = \sigma_{ey}$ and the antiproton beams, $\sigma_{px} = \sigma_{py}$) and the electron beam transverse emittance to be much larger than both the electron and antiproton beam longitudinal emittances (typical during operation), the cooling rate, defined as the time derivatives of the emittances, depends on the angles (or transverse velocities) as $\sigma_{ex}^{-2}$ for the longitudinal direction and $\sigma_{ex}^{-3}$ for the transverse. Therefore, cooling efficiency is very sensitive to variations of the angle value.

The origins of the angles can be roughly divided into four categories:

- incoherent angles originated from the thermal electron velocities at the cathode (57 μrad)
- angles resulting from an envelope mismatch (~50 μrad)
- nonlinearities in the beam line (from the external, ~20 μrad, or self fields, $\lesssim$ 10 μrad)
- coherent dipole motion (~55 μrad)

Estimates in parenthesis are for a 0.1-A beam with the values of the angles obtained from averaging over the transverse section of the beam, which radius is assumed to be 2 mm. The total angle (1D, rms) was then estimated to be ~100 μrad (contributions summed in quadrature).

A peculiarity of the Recycler is to share the same tunnel as the MI synchrotron. Hence, shielding of the cooler entire beam line was critical to minimize the effects of the MI busses stray fields, both on the cooling section and the rest of the beam line, where the electron beam would be displaced by tens of millimetres when the MI was ramping up and down. Also, the Beam Position Monitors (BPM) were biased in order to prevent ions (from beam-background gas interactions) to be captured in the electron beam potential well.

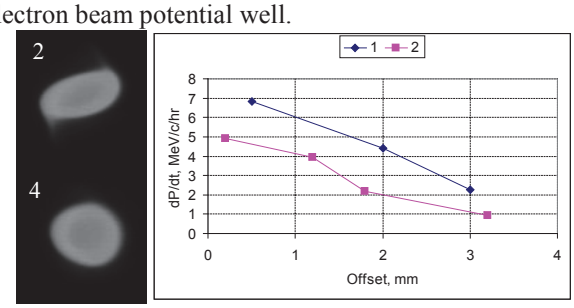


Figure 2: (Left) Images of the beam with zero (top) and optimized (bottom) quadrupole currents ($I_e$ ~ 0.1A, 2μs pulse); (Right) Longitudinal cooling rates at various vertical offsets of the electron beam before (set 2) and after (set 1) adjustments of quadrupoles ($I_e$ = 0.1 A).

Initial tuning (or matching) of the beam shape and size in the cooling section was made by measuring the envelope with round apertures (i.e. scrapers) positioned in between the solenoid modules and adjusting the two lenses directly upstream of the cooling section [11]. This was sufficiently efficient to demonstrate cooling and for early operation. However, in this procedure, the beam boundary is determined by scraping ~$10^{-5}$ of the beam intensity. Therefore, it was sensitive only to the beam halo, which properties may be very different from the core's [12]. Eventually, direct imaging in a pulse mode with a scintillator clearly revealed that the beam core was elliptical [13] (Fig. 2), which would explain the relatively poor cooling rates at the beginning of operation.

## COOLING OPTIMIZATION

Drag rate measurements were used to optimize the cooling performance. The drag rate, $\dot{\bar{p}}$, here measured by



ISBN 978-3-95450-140-3

the 'voltage jump' method [14] (similar to [15]), represents the longitudinal cooling force averaged over all antiprotons. Hence, to interpret a drag rate as a cooling force experienced by the central particle, the antiproton beam needs to have a small rms momentum spread and a small transverse emittance.

Thus, in order to obtain reliable and reproducible measurements, the transverse emittance must remain low throughout the measurement period. To do so, it was necessary to: keep the transverse stochastic cooling system on during the measurements; scrape the antiproton beam down to the limit at which a reasonable resolution of the Schottky detector remained, $N_p \sim 1\times10^{10}$; and apply the strongest cooling between measurements. The reproducibility of the results was also improved by progressively reducing the electron angles spread across the beam (i.e. improving the beam quality).

Figure 3 shows the dependence of drag rates on the beam current recorded over the years. The significant enhancement of the cooling force came mainly from three improvements that decreased the electron angles in the cooling section.

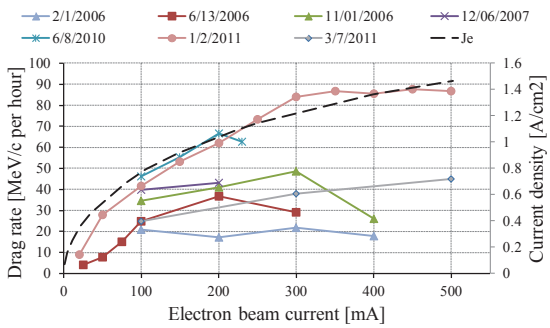


Figure 3: Drag rate as a function of the beam current measured on axis at various dates with a 2 kV voltage jump. The current density calculated at the beam centre (dashed curve) is shown for comparison. Note that the flattening of the best curve on Figure 3 (labelled '1/2/2011'), at about 80 MeV/c per hour, is, at least partly, the result of the measurement procedure being inadequate for large drag rates.

First, focusing was optimized by adjusting the corrector quadrupoles based on drag rate measurements at the electron beam periphery [16]. Figure 2 shows the corresponding improvements for measurements of the cooling rate.

Second, a beam-based procedure for aligning the magnetic field in the cooling section was developed [17]. The displacement of ten CS's individual modules with respect to one another due to the ground motion effectively introduces an undesirable transverse component to the field, which needed to be compensated at regular intervals (~twice a year) to preserve optimum cooling.

Finally, the electron angles were found to be affected by ions created by the electron beam and captured by its own space charge. While there were many ion clearing electrodes along the beam line, the remaining ion neutralization ~2% still significantly affected focusing for beam currents $\gtrsim$ 100 mA. The remedy to decrease the average ion concentration was to apply periodic interruptions of the electron beam (2 μs with a frequency up to $f_{int}$ = 100 Hz depending on the beam current; so-called ion clearing mode) allowing ions to drift toward the biased electrodes or vacuum chamber [18].

The cooling rate defined as the difference of the time derivative of the momentum/emittances with the cooling system on and off, assesses numerically its actual effectiveness for operational conditions. The standard measurement procedure is described in Ref. [19]. Figure 4 summarizes electron cooling rates between 2006 and 2010. Over that time, the cooling rate for a given transverse emittance significantly increased due to the improvements to the electron beam quality discussed previously. The arrows indicate the observed rate increase resulting from each of these beam optimization steps.

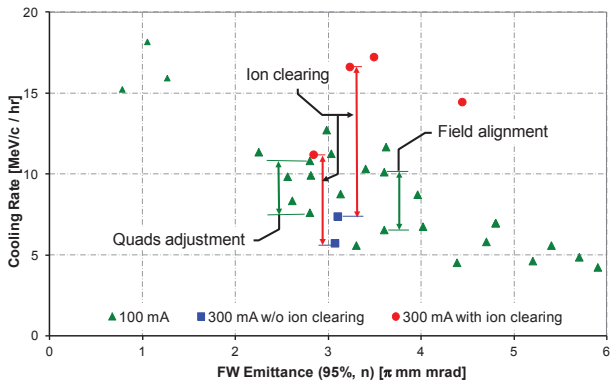


Figure 4: Longitudinal cooling rates (negated) in 2006-2010.

## OPERATION

In all previous electron coolers, electron and antiproton beams were overlapping concentrically. In the Recycler cooler, this configuration, which yields the maximum cooling rate, was not always required and induced a strong deterioration of the antiprotons lifetime. The solution to alleviate the latter was to displace the electron beam trajectory with respect to the antiproton beam orbit and adjust this offset to obtain the needed cooling. Typically, strongest cooling was only applied when preparing the antiprotons for extraction to the Tevatron.

One operational difficulty was energy drifts (mentioned above). Keeping the equipment temperatures as constant as possible was found to be critical. Also, the parameters of the energy regulation loop were periodically corrected based on the shape of the Schottky momentum distribution of the antiprotons, which is very sensitive to the momentum difference between the two beams. A momentum mismatch is characterized by a flat profile of the distribution near its maximum (Fig. 1b, red trace), while the Schottky profile becomes 'peaky' or triangular when energies are matched (Fig. 1b, blue trace).

When electron cooling was fully optimized and the ion clearing mode operational, the ability to apply strong

ISBN 978-3-95450-140-3

cooling revealed two expected limitations: a transverse instability of the antiprotons with very small emittances and lifetime deterioration.

An impedance-driven beam instability [20] was predicted and transverse dampers were designed and implemented, greatly extending the stability region during accumulation. However, the extraction process includes complicated manipulations in the longitudinal phase space, and instabilities were observed a few times [21 and references therein]. An illustration of the instability on a single bunch during extraction is shown in Fig. 5.

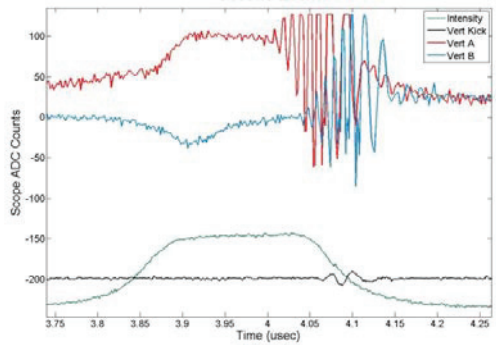


Figure 5: Instability of a single bunch during extraction. Oscillation frequency is ~100MHz.

In the Recycler, where antiprotons are typically accumulated for ~15 hours, preserving the antiproton beam lifetime is crucial. Although, we have not found a single parameter or combination of parameters that would uniquely determine the lifetime, it was observed, for instance, that the lifetime would increase quite significantly when increasing the bunch length. Correspondingly, the data collected seems to favour the linear density rather than the transverse emittance as the beam parameter most likely to correlate with the value of the beam lifetime.

In addition, while applying strong electron cooling deteriorates the lifetime, stochastic cooling improves it. A possible interpretation is that stochastic cooling acts on the far tail particles that electron cooling induces (probably similar to what is known as 'electron heating' for low-energy coolers [22]). Thus, from an operation point of view, it was very important to keep the stochastic cooling system properly tuned, even though its effect on the measured emittance of large stacks was insignificant.

## FINAL PERFORMANCE

Ultimately, the Recycler performance is characterized by its ability to store antiprotons efficiently and deliver bunches with adequate beam parameters to the Main Injector/Tevatron. In order to quantify the efficiency of the Recycler as a repository of antiprotons overall, a storage efficiency can be defined [23]. It includes injection and extraction efficiencies from and to the Main Injector, losses due to the antiprotons lifetime and accidental losses (e.g.: correctors' power supply trip, vacuum burst, and instability). For a typical accumulation and extraction cycle, where there is no accidental loss or operational issue, the storage efficiency was ~93%. Out of the 7% of beam which is lost, ~4% is due to injection and extraction inefficiencies while ~3% come from the antiprotons lifetime. At the same time, the Recycler was able to consistently cool the antiprotons to the adequate emittances (typically, 70 eV·s and 3 μrad, 95%, normalized), and deliver them to the Main Injector without deteriorating the quality of the bunches.

## ACKNOWLEDGEMENTS

The success of electron cooling at Fermilab came as the result of efforts from many dedicated individuals, who cannot be listed here. Authors are thankful to all of them.

## REFERENCES

[1] G. Jackson, "The Fermilab Recycler Ring Technical Design Report", FERMILAB-TM-1991 (1996)
[2] S. Nagaitsev *et al.*, Phys. Rev. Lett. **96**, 044801 (2006)
[3] A. Burov *et al.*, PRSTAB **3** 094002 (2000)
[4] J. A. MacLachlan *et al.*, "Prospectus for an electron cooling system for the Recycler," FERMILAB-TM-2061 (1998)
[5] A. Shemyakin, L.R. Prost, COOL'11, Alushta, Ukraine (2011) 31 (THIOA01)
[6] Pelletrons are manufactured by the National Electrostatics Corporation, www.pelletron.com
[7] A. Sharapa *et al.*, NIM-A 417 (1998) 177
[8] L.R. Prost and A. Shemyakin, Proc. of PAC'05, Knoxville, USA (2005) 2387
[9] S. M. Seletskiy and A. Shemyakin, Proc. of PAC'05, Knoxville, USA (2005) 3638
[10] Ya.S. Derbenev, A.N. Skrinsky, Particle Accelerators **8** (1977) 1
[11] T.K. Kroc *et al.*, Proc. of PAC'05, Knoxville, USA, (2005) 3801
[12] A. Burov *et al.*, Proc. of COOL'05, Galena, USA (2005) 139
[13] A. Shemyakin, *et al.*, Proc. of PAC'09, Vancouver, Canada (2009), TU6PFP076
[14] L. Prost *et al.*, ICFA-HB'06, Tsukuba, Japan, (2006) 182 (WEAY02)
[15] G.I. Budker *et al.*, Preprint IYaF 76-32 (1976)
[16] A. Shemyakin *et al.*, PAC'09, Vancouver, Canada (2009) 1466 (TU6PFP076)
[17] L.R. Prost, A. Shemyakin, COOL'07, Bad Kreuznach, Germany (2007) 179 (THAP09)
[18] A. Shemyakin *et al.*, Proc. of IPAC'10, Kyoto, Japan (2010) MOPD075
[19] L.R. Prost, A. Shemyakin, PAC'07, Albuquerque, NM (2007) 1715 (TUPAS030)
[20] A. Burov & V. Lebedev, PRSTAB **12** 034201 (2009)
[21] L.R. Prost *et al.*, PAC'11, New York, NY (2011) 1698 (WEP114)
[22] L. Hermansson, D. Reistad, Nucl. Inst. & Methods Phys. Res. A **441** (2000) p.140
[23] L.R. Prost *et al.*, COOL'09, Lanzhou, China (2009) 1 (MOM1MCIO01)



ISBN 978-3-95450-140-3